



Faculty & Staff Scholarship

2003

Alcohol Synthesis over Pre-Reduced Activated Carbon-Supported Molybdenum-Based Catalysts

Xianguo Li
Ocean University of China

Lijuan Feng
Ocean University of China

Lijun Zhang
Ocean University of China

Dady B. Dadyburjor
West Virginia University

Edwin L. Kugler
West Virginia University

Follow this and additional works at: https://researchrepository.wvu.edu/faculty_publications

Digital Commons Citation

Li, Xianguo; Feng, Lijuan; Zhang, Lijun; Dadyburjor, Dady B.; and Kugler, Edwin L., "Alcohol Synthesis over Pre-Reduced Activated Carbon-Supported Molybdenum-Based Catalysts" (2003). *Faculty & Staff Scholarship*. 2881.

https://researchrepository.wvu.edu/faculty_publications/2881

This Article is brought to you for free and open access by The Research Repository @ WVU. It has been accepted for inclusion in Faculty & Staff Scholarship by an authorized administrator of The Research Repository @ WVU. For more information, please contact ian.harmon@mail.wvu.edu.



Alcohol Synthesis over Pre-Reduced Activated Carbon-Supported Molybdenum-Based Catalysts

Xianguo Li ^{1,*}, Lijuan Feng ¹, Lijun Zhang ¹, Dady B. Dadyburjor ² and Edwin L. Kugler ²

¹ College of Chemistry and Chemical Engineering, Ocean University of China, Qingdao, Shandong 266003, P. R. China

² Department of Chemical Engineering, West Virginia University, P.O. Box 6102, Morgantown, West Virginia 26506-6102, U.S.A. E-mail for Prof. Dadyburjor: Dady.Dadyburjor@mail.wvu.edu; E-mail for Prof. Kugler: Edwin.Kugler@mail.wvu.edu

* Author to whom correspondence should be addressed. Tel. (+86)-532-2032482-8318, Fax: (+86)-532-2032483, E-mail: lixg@mail.ouqd.edu.cn

Abstract: Activated carbon (AC)-supported molybdenum catalysts, either with or without a potassium promoter, were prepared by the incipient wetness impregnation method. The materials were characterized using differential thermal analysis (DTA) and temperature programmed reduction (TPR), and were used for mixed alcohol synthesis from syngas (CO+H₂). DTA results showed that a new phase, related to the interaction between Mo species and the AC support, is formed during the calcination of the Mo/AC catalyst, and the introduction of a K promoter has noticeable effect on the interaction. TPR results indicated that the Mo is more difficult to reduce after being placed onto the AC support, and the addition of a K promoter greatly promotes the formation of Mo species reducible at relatively low temperatures, while it retards the generation of Mo species that are reducible only at higher temperatures. These differences in the reduction behavior of the catalysts are attributed to the interaction between the active components (Mo and K) and the support. Potassium-doping significantly promotes the formation of alcohols at the expense of CO conversion, especially to hydrocarbons. It is postulated that Mo species with intermediate valence values (averaged around +3.5) are more likely to be the active phase(s) for alcohol synthesis from CO hydrogenation, while those with lower Mo valences are probably responsible for the production of hydrocarbons.

Keywords: Alcohol synthesis, molybdenum; activated carbon; DTA; TPR.

Introduction

Unsupported or supported molybdenum-based catalysts have been widely employed in the petroleum industry and for hydrotreating [1]. Oxides, such as alumina, silica, silica-alumina, are commonly used as the supports for these purposes, and for the synthesis of hydrocarbons [2-4] and alcohols [5-8] from carbon monoxide (or dioxide) and hydrogen. A carbon support has also been used for hydrocarbon synthesis [9] and higher alcohol synthesis [10-13] from CO and H₂. The synthesis of alcohols, especially higher alcohols (ethanol and higher), has come to be a focus of interest in the past decades owing to the increasing demand of octane boosters of gasoline for the sake of environmental protection.

The direct synthesis of higher alcohols from synthesis gas (syngas, CO+H₂) has been extensively reviewed by Klier et al. [14] and by Forzatti et al. [15]. It is widely recognized that higher alcohols together with methanol (MeOH) can be produced from syngas by appropriate modification of MeOH-synthesis catalysts and the reaction conditions [16-25]. Over the catalysts in this category, a significant amount of isobutanol is often produced. In the 1970s and 1980s, researchers at Union Carbide Corporation extensively explored soluble Rh and Ru complexes, either with or without promoters, as homogeneous catalysts for the production of oxygenates [26-33], including methanol, ethanol, and especially ethylene glycol. The principal shortcoming of all homogeneous CO hydrogenation reactions is their low catalytic activity, which results in the need to use high catalyst loadings and drastic reaction conditions (usually at temperatures above 200°C and pressures above 30MPa) [34]. Rh- and Ru-based heterogeneous catalysts have also been used for the synthesis of higher oxygenates [5, 35, 36]. Classical Fischer-Tropsch (F-T) catalysts have also been modified, by addition of alkali-metal compounds or by nitridation, to improve the selectivity toward alcohols [37]. It was also claimed that mixtures of alcohols could be produced with high activity and selectivity over a series of materials consisting of MeOH-synthesis catalysts and F-T catalysts [38].

The final category of catalysts for the synthesis of higher alcohols is promoted Mo-based materials. Molybdenum sulfides promoted by alkali-metal compounds (and optionally promoted by cobalt) have drawn considerable interests [10-13, 39-48] ever since the scientists at Dow Chemical [49,50] and Union Carbide [51] discovered that these materials are active for the production of C₁ to C₅ alcohols, and that they are resistant to sulfur.

On the other hand, however, pre-reduced (rather than sulfided) Mo-based catalysts received less attention. Tatsumi et al. [6-8] systematically investigated alcohol synthesis over pre-reduced Mo-based catalysts supported on various oxides, with special emphasis on the effects of supports and 3d transition metals. The results showed that a Mo-Ni-K/SiO₂ catalyst performed the best with a space-time yield to total alcohols of up to 420 g/h/kg of catalyst [8]. Alyea et al. [52] studied alcohol synthesis performance on reduced Mo-Ni-K (or Cs)/SiO₂ catalysts prepared by a special MOVS (Metal Oxide Vapor Synthesis) method. The performance was compared with that on conventionally impregnated catalysts. The study showed that MOVS catalysts performed better. More recently, Storm [53] investigated the effect of Co and Rh promoters on alcohol synthesis performance over pre-

reduced Mo-K/ γ -Al₂O₃ catalysts. It was claimed that the addition of a Rh promoter to the catalyst increased the space-time yield of alcohols from 370 to 1100 g/h/kg of catalyst.

Most of the previous work on pre-reduced Mo-based catalysts used for alcohol synthesis dealt with unsupported or oxide-supported materials. It is reasonable to expect that the catalytic performance depends, to a certain extent at least, on the support used since the surface property of the catalyst varies with the support. Carbon-supported materials have been claimed to have some potential advantages over oxide-supported ones, such as lower tendency of carbon deposition [54], less dehydration and thus less secondary reactions of alcohol products. In our previous studies [45, 46], we have carried out detailed investigations on alcohol synthesis over vapor phase synthesized MoS₂ catalysts and carbon-supported sulfided Mo-based materials. Here, we present results on alcohol synthesis over H₂-prereduced carbon-supported Mo-based catalysts. The effect of a potassium promoter is presented. The catalytic performance is partly correlated with the property change of the catalysts during the preparation and pretreatment process.

Results and Discussion

Property changes during the catalyst calcination process

The property changes of the catalysts during the calcination process was investigated by means of DTA technique. Figure 1 shows the DTA curves of the calcined and dried AC supports. There is only one endothermic peak at around 83°C for both samples. The peak is contributed to the desorption of the adsorbed water. It is not surprising that the peak appears even after the samples being dried or calcined in view of the fact that AC is an excellent adsorbent with very high capacity and high adsorbing rate. No distinct difference was seen between the DTA curves of the two samples, suggesting that calcination has essentially no effect on the thermal property of the support.

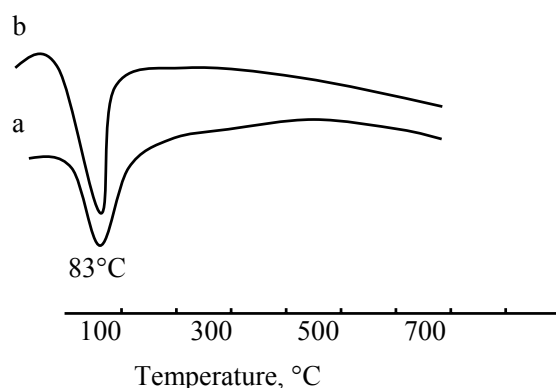


Figure 1. DTA curves of the activated carbon support. Samples are as follows: (a) calcined sample; and (b) as-is material.

The DTA curve of the AHM is shown in Figure 2. Since the sample was dried at 120°C prior to the experiment, there was no peak corresponding to the desorption of water. Instead, there were three endothermic peaks located at 210°C, 250°C and 400°C, respectively. The first two peaks are owing to the dehydration of the crystal waters in the polymolybdate. The third peak may correspond to the decomposition of the sample to produce MoO₃. The result is consistent with that reported in a thermal gravity analysis [56].

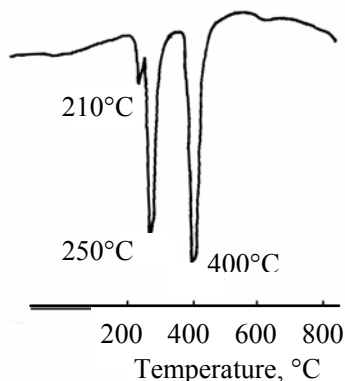


Figure 2. DTA profile of ammonium heptamolybdate.

Figure 3 presents the DTA curves of a few Mo-based catalysts. It is seen from the figure that the DTA curves of the calcined catalysts, either with or without a K promoter, are very similar to one another and to that of the support itself, suggesting that a K promoter has basically no effect on the thermal property of the catalyst. It is also an indication that the catalyst is fairly stable after calcination.

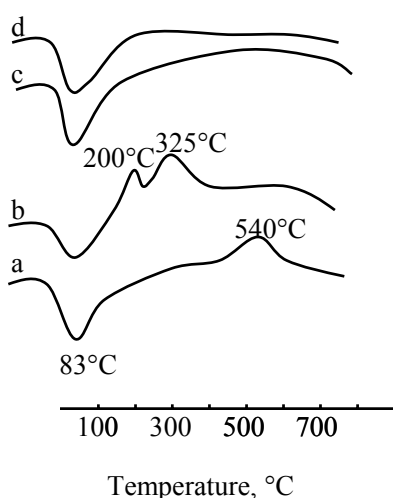


Figure 3. DTA spectra for activated carbon-supported molybdenum-based catalysts. Samples are as following: (a) Mo(18)/AC(D); (b) Mo(18)-K(1.2)/AC(D); (c) Mo(18)/AC(C); and (d) Mo(18)-K(1.2)/AC(C).

On the other hand, however, the DTA curves of the dried catalysts are obviously different from those of the calcined ones. One or two exothermic peaks were generally observed for the dried catalysts, while there was no endothermic peak corresponding to the stepwise dehydration and/or the decomposition of the AHM (or the decomposition of KNO_3). The reason might be that the exothermic peak(s) concealed the endothermic effect because of the low concentrations of the components (Mo and K).

The presence of an exothermic peak at about 540°C in the DTA curve of catalyst Mo(18)/AC(D) is an indication of the formation of a new phase in the catalyst at this temperature. This exothermic peak is not seen in either the DTA curve of the AC support or the DTA curve of the AHM. Therefore, it is believed that the formation of the new phase is related to the interaction between the Mo species and the support.

Ratnasamy and co-workers studied the structure change of Co-Mo/ γ -(or η -) Al_2O_3 catalysts for hydrodesulfurization during the calcination process by using DTA and X-ray analysis [57]. The DTA result indicated that there occurred an interaction between Mo species and the support, thus leading to the formation of a new phase. The conclusion was supported by X-ray analysis. They also found that the presence of Co retarded this change, leading to a 40°C upward shift of the exothermic peak.

Compared with γ -(or η -) Al_2O_3 , the surface of AC is relatively inert, but oxygen-containing functional groups still exist [58]. Therefore, it is possible that the active components of a catalyst interact with those groups when they are dispersed onto the surface of the AC support, especially at higher temperatures. The only difference is that the interaction might be weaker.

When potassium was introduced into the catalyst, the exothermic peak at around 540°C disappeared. Instead, two other exothermic peaks appear at about 200°C and 325°C . The reason may be multifold. The first possibility is that the introduction of K promoted the interaction between the Mo species and the support, leading the interaction occurs at lower temperatures, and consequently resulting in a downward shift of the exothermic peak. It is also possible that the K promoter interacts with Mo as well as AC support, leading to the formation of (a) new K-Mo-C phase(s).

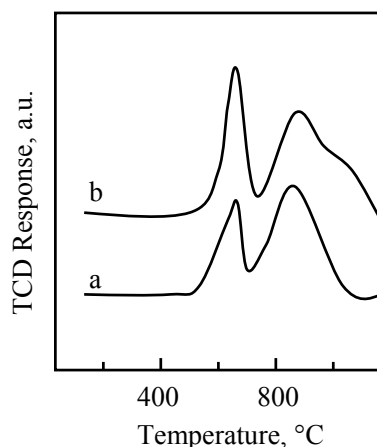


Figure 4. TPR spectra of bulk MoO_3 (a) made-in-house, and (b) commercially obtained.

In view of the fact that no distinct exothermic peak appears in any of the DTA curves of the calcined catalysts, it is believed that the interaction among the active components (Mo, K) and the support occurs during the calcination process rather than any other preparation step.

The reduction behavior of the catalysts

The reduction behavior of the AC-supported Mo-based catalysts was studied by means of TPR technique, and has been reported elsewhere in detail [55]. Results are briefly presented and discussed below, with special emphasis being on the relationship between these results and DTA data as well as the catalytic performance to be presented later.

Reduction of bulk MoO₃

The reduction of a commercially obtained MoO₃ (from Aldrich Chemical Company) and a sample prepared by thermolysis of AHM in flowing N₂ at 500°C for 2h has been examined first. The TPR profiles of both samples, as seen in Figure 4, show two H₂ consumption peaks: one at a temperature around 660°C, and the other at 850°C. The shape and the location of the two peaks are very similar for the two samples, suggesting that AHM is converted to MoO₃ after calcination in flowing N₂ at 500°C. The ratio of the area of the high-temperature peak to that of the low-temperature peak is approximately 2. Furthermore, the average Mo valence values after the low- and high-temperature reduction, calculated from the H₂ consumption, are close to +4 and 0, respectively (+3.86 and -0.26 for commercially obtained MoO₃, and +3.92 and -0.20 for the MoO₃ prepared in-house). These results suggest that the reduction of bulk MoO₃ consists of two distinct steps as follows:



Metallic Mo is obtained after the whole TPR run. This is in agreement with the literature results [59, 60].

Reduction of the AC support

The TPR profile of the AC support is shown in Figure 5b. Curve 5a was obtained by heating the AC support in pure Ar (rather than in a H₂/Ar mixture) following the same temperature program as in a TPR run. In other words, this was a temperature-programmed desorption (TPD) run, rather than a TPR. The TPR profile (curve 5b) exhibits a positive peak at a temperature around 570°C and a negative peak at about 850°C. The positive peak must be the reduction of the oxidized surface of the AC support and/or some of its impurities (as indicated by ICP results). The negative peak is attributed to the desorption of CO from the decomposition of the oxidized carbon support.

It is well known that carbon surfaces can chemisorb oxygen at low temperatures (e.g., near room temperature), resulting in the formation of oxygen-containing surface complexes of varying thermal stability [61]. It is also recognized that once oxygen is chemisorbed it can only be removed as an oxide of carbon (CO and CO₂) when the carbon is subjected to heat in vacuum or in a non-oxidative

atmosphere [58, 62-64]. Any CO released would pass through the dry ice/acetone trap with CO₂ removed. Since the thermal conductivity of CO is greater than that of Ar, the thermal conductivity of the effluent gas mixture would increase, causing a negative peak in the TPR or TPD spectrum. Further, since some of the oxygen on the surface reacts with H₂ at lower temperatures (giving positive peaks) in a TPR experiment, less oxygen remains at higher temperatures for AC decomposition to form CO and CO₂. Therefore, a smaller negative peak should be observed in a TPR experiment than in a TPD. That was in fact observed.

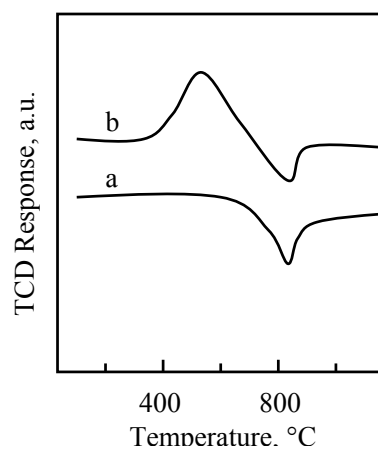


Figure 5. Spectra for activated carbon support: (a) TPD curve in pure Ar; and (b) TPR profile in H₂/Ar gas mixture.

Reduction of K/AC(C) samples

The TPR spectra of K/AC(C) samples with different K loadings are shown in Figure 6. Also included in the figure is the TPR profile of the AC support itself. Qualitatively, they are consisted of one or two positive peak(s) and a negative peak.

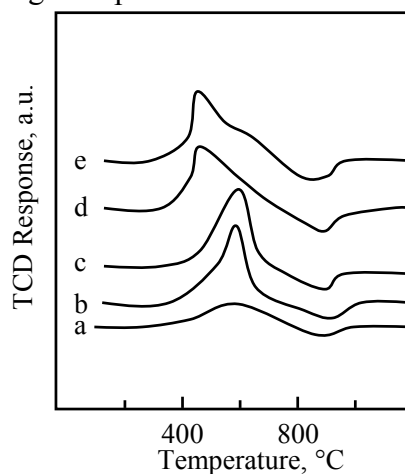


Figure 6. TPR spectra of the K/AC(C) samples with K loadings of (a) 0%, (b) 2.9%, (c) 5.8%, (d) 8.8%, and (e) 11.6% by weight, respectively.

As mentioned earlier, the negative peak is contributed to CO desorption from AC support. The positive peak(s) can still be assigned to the reduction of the AC support itself. This can be explained as follows. The total area [of the positive peak(s)] under the TPR spectrum, corresponding to the amount of H₂ consumed, increases significantly even when less than 3wt% of K is added. However, addition of over 11wt% K does not increase the H₂ consumption very much beyond the initial increase. This is clearly an indication that the K itself is not reduced, but may modify the reduction of (the impurities in) the carbon support. Kelemen etc. drew similar conclusions from their UPS measurement studying KOH adsorbed on graphite surfaces [63, 65].

Reduction of Mo-based catalysts

Based on the above-described preliminary studies, we further investigated the reduction behavior of catalysts Mo(18)/AC(C) and Mo(18)-K(1.2)/AC(C). Their TPR spectra are given in Figure 7. The TPR curve of the AC support is also included in the figure for comparison. Qualitatively, the TPR profile of catalyst Mo(18)/AC(C) consists of two positive peaks, one shoulder and one negative peak, while the TPR curve of catalyst Mo(18)-K(1.2)/AC(C) is comprised of one positive peak, one shoulder and one negative peak. The designation of the negative peak has been described earlier. Detailed discussion follows only for the positive peak(s).

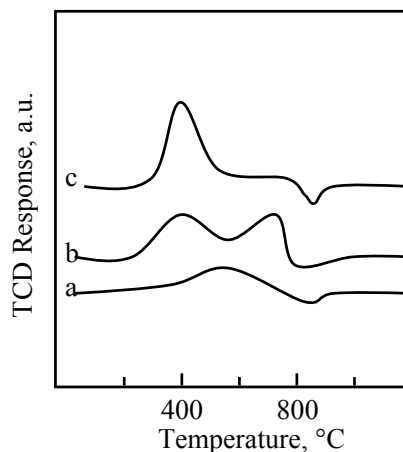


Figure 7. TPR profiles of (a) activated carbon support, (b) catalyst Mo(18)/AC(C), and (c) catalyst Mo(18)-K(1.2)/AC(C).

Our previous study [55] has shown that the profiles can be generally deconvoluted into four positive peaks. Considering that potassium is not reduced itself while it modifies the reducibility of other components in the catalysts, we applied the same deconvolution procedure to both of the catalysts. The result is illustrated in Figure 8. The four peaks are denoted as Peaks X, Y, S and Z, located at around 350, 450, 550 and 700°C, respectively. Peak S is attributed to the reduction of the support itself (and/or some of its impurities), as a similar peak also appears at about the same temperature in the case of the support alone. The other three peaks are contributed to the reduction of different Mo species on the

support. Peaks X and Y are grouped together as low-temperature peaks, with peak Z being the high-temperature peak. This is different from the case with oxides as the supports. In the latter case, one low-temperature peak and one high-temperature peak, contributed to the reduction of octahedrally and tetrahedrally coordinated Mo species [denoted as Mo(O) and Mo(T)] respectively, are usually observed [1, 66, 67]. This is an indication that the distribution of Mo species in C-supported Mo-based catalysts is more complicated than that in oxide-supported ones.

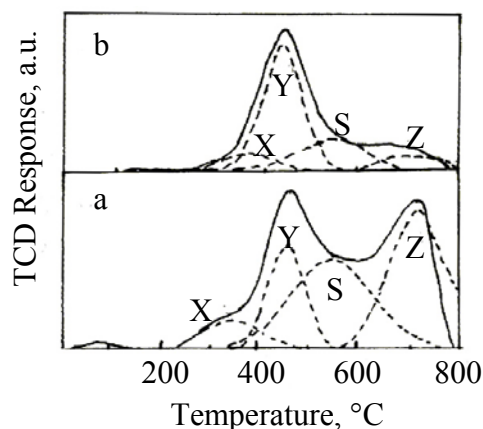


Figure 8. The deconvolution results of the TPR profiles for (a) catalyst Mo(18)/AC(C), and (b) catalyst Mo(18)-K(1.2)/AC(C). Solid and dotted lines are for experimental and fitted curves, respectively.

For Mo(18)/AC(C) catalyst, the average Mo valence values after low- and high-temperature reduction are +5.02 and +2.36 respectively. The ratio of the total area of the two low-temperature peaks to the area of the high-temperature peak is 0.49. Compared with the reduction of bulk MoO₃, it can be seen that Mo is more difficult to be reduced after being supported onto the AC support. The Mo can not be reduced to metallic state after the whole TPR run. This is also different from the case with oxides as the supports. For oxide-supported Mo-based catalysts, Mo is usually completely reduced to metal at about 800°C [66].

Recall that interaction occurs between Mo species and the AC support during the calcination process, it is reasonable to contribute the different reduction behavior of the AC-supported Mo catalyst (from that of bulk MoO₃) to the interaction.

For catalyst Mo(18)-K(1.2)/AC(C), the presence of K pronouncedly modifies the reduction behavior of Mo species. This can be qualitatively seen from Figure 7. Quantitative result shows that the average Mo valence values after low- and high-temperature reduction are +3.46 and +2.93, respectively, and the ratio of the total area of the low-temperature peaks to the area of the high-temperature peak is 4.76. That is to say, at relatively lower temperatures, most of Mo present in the catalyst is reduced to Mo species with intermediate valence value (averaged about +3.5) and most of it

cannot be reduced any further. This obviously indicates that the introduction of K greatly promotes the formation of Mo species reducible at lower temperatures, while it retards the generation of Mo species reducible only at higher temperatures. Molybdenum is also not completely reduced after the whole temperature run. Again, these differences in the reduction behavior of the K-promoted catalyst may have some relation with the above-mentioned modification effect of potassium on the interaction between the active components and the support.

From the above results, it can be inferred that the introduction of K leads to the Mo in the catalyst more easily being reduced to Mo species with intermediate valence value, while prevents the further reduction of Mo.

Catalytic performance

Two catalysts, Mo(18)/AC(C) and Mo(18)-K(1.2) /AC(C), were tested for alcohol synthesis performance. Results are presented in Figures 9 and 10.

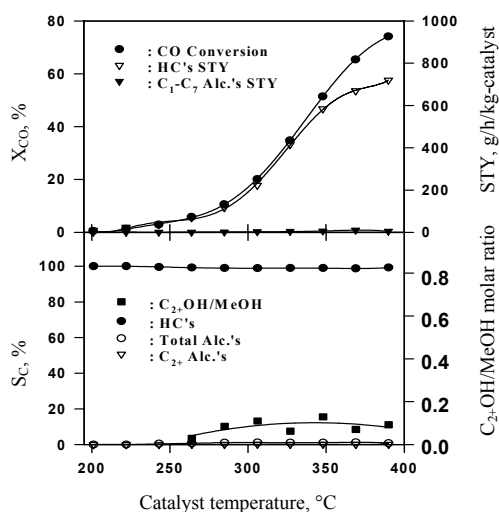


Figure 9. Catalytic performance of catalyst Mo(18)/AC(C) for CO hydrogenation. The following parameters are reported: X_{CO} , the conversion of CO; STY, space-time-yield; S_C , CO₂-free carbon atom-selectivity; and C₂₊OH/MeOH, the molar ratio of higher alcohols to methanol. **Reaction conditions** are: 0.5g of catalyst; $p=5.1$ MPa (750 psig); H₂/CO molar ratio=1; GHSV=6 m³/h/kg of catalyst.

It is obvious from Figure 9 that the catalyst without potassium doping is very active for CO hydrogenation, while the predominant products are light hydrocarbons. In fact, methanol and ethanol are the only two alcohol products observed, and they are present in vanishingly small amounts. These results are in agreement with those observed on H₂-reduced Mo/SiO₂ catalysts [6, 8]. They are also

consistent with the results obtained on molybdenum sulfide catalysts [14, 39, 42, 43, 45, 46, 49, 51], either supported or unsupported.

For the K-promoted catalyst, with increasing temperature, the following dependence of the catalytic performance was observed: a monotonic increase in the overall CO conversion and in the STY (Space Time Yield) of hydrocarbons, a maximum for the STY of the total alcohols, a minimum in the CO₂-free carbon atom-selectivity to hydrocarbons, a maximum for the selectivity to the total alcohols and for the selectivity to higher alcohols, and a monotonic increase in the molar ratio of higher alcohols to methanol. (Note that at lower temperatures, no alcohol product was obtained. Therefore, no data on the molar ratio of higher alcohols to methanol are reported.) The postulation that the activation energy for methanol synthesis is lower than that for the formation of higher alcohols and hydrocarbons [39, 68] may help to explain some of these observations.

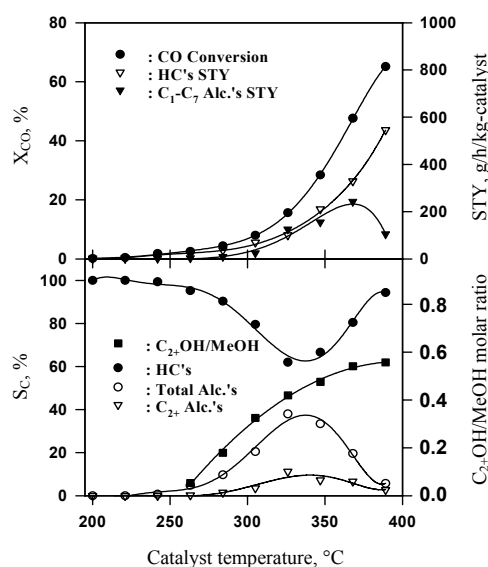


Figure 10. Catalytic performance of catalyst Mo(18)-K(1.2)/AC(C) for the synthesis of mixed alcohols from syngas. Catalyst parameters and reaction conditions are the same as in Figure 9.

With the addition of a potassium promoter, dramatic changes in the catalytic performance are clearly noted. As seen in Figure 10, the overall CO conversion decreases slightly, from 74% to 65% at the highest temperature studied. The STY of hydrocarbons shows a parallel decline, from about 720 to around 550 g/h/kg of catalyst at the highest temperature. Most of all, the formation of alcohols is greatly promoted by the K-doping. For the undoped catalyst (Figure 9), the STY of total alcohols is essentially zero if the reactivity of the reactor tube itself [46] is taken into account. However, for the K-promoted catalyst, the highest STY of total alcohols (at approximately 370°C) approaches 250 g/h/kg of catalyst. Further, with the addition of potassium, the CO₂-free carbon atom-selectivities to total alcohols and to C₂₊ alcohols increase pronouncedly, reaching the highest of about 40% and 10%

(at about 340°C), respectively, at the expense of the selectivity to hydrocarbons. The molar ratio of higher alcohols to methanol also increases significantly with the addition of potassium. It is also clear that the effect of the potassium promoter on the catalytic performance is especially pronounced at higher temperatures, i.e. temperatures higher than 250°C.

By correlating these results with the reduction behavior described earlier, it is postulated that Mo species with intermediate valence (averaged around +3.5) are more likely to be the active phase(s) for alcohol synthesis from CO hydrogenation, while those with lower Mo valence are probably responsible for the production of hydrocarbons. This is in general agreement with the study by Tatsumi et al. [8] who investigated the synthesis of mixed alcohols over H₂-prereduced SiO₂-supported Mo-based catalysts.

Summary and Conclusions

The production of mixed alcohols from synthesis gas was investigated on H₂-prereduced AC-supported Mo-based catalysts. The precursor catalysts were prepared by incipient wetness impregnation method and were characterized by DTA and TPR techniques. The characterization shows that interaction between the active components (Mo, K) and the support occurs during the calcination process of the catalysts. The interaction is responsible for the different reduction behavior, which leads to different catalytic performance for CO hydrogenation. It is believed that Mo species with intermediate valence values are more likely to be the active phase(s) for alcohol synthesis, while those with lower Mo valences are probably responsible for the production of hydrocarbons.

Acknowledgements

This work was supported by the US Department of Energy under Contract No. DE-AC22-91PC91034. X. Li and L. Feng thank the Scientific Research Foundation for the Returned Overseas Chinese Scholars, Ministry of Education of China for the partial sponsorship to the work.

Experimental

Catalyst preparation

Activated carbon (AC) support was obtained from Aldrich Chemical Company. The granule size of the AC support is 20-40 mesh; the specific surface area is 660m²/g, and the pore volume is 1.0 mL/g. ICP results indicate that impurities present in the support are: Si 8.0%, Al 0.87%, Fe 0.28%, Ca 0.18%, Mg 0.074%, Ba 0.069%, smaller amounts of Sr and Ti, and at least six other metals in the ppm range. (Data cited are in weight percentage with accuracy of ± 50% of the amount present.)

The catalysts were prepared by step-wise incipient wetness impregnation method with ammonium heptamolybdate [(NH₄)₆Mo₇O₂₄·4H₂O, AHM] and potassium nitrate (KNO₃) being the sources of Mo and K respectively. For dried samples (denoted as D), drying in air at 100°C overnight was the only

step following each impregnation step of the active component (Mo) or the K promoter; while for calcined samples (denoted as C), calcination in flowing N_2 at a certain temperature ($500^\circ C$ for Mo and $300^\circ C$ for K) for 2h was also performed after each drying step. Details about the preparation of the catalysts were given elsewhere [55].

Molybdenum loading is presented as nominal Mo mass percentage relative to AC support, while the concentration of the K promoter is given as its molar ratio to Mo. These aspects of catalyst preparation along with the impregnation sequence of the components are represented in the designation code. For example, Mo(18) -K(1.2)/AC(C) denotes a calcined catalyst with a Mo loading of 18 mass% and a K/Mo molar ratio of 1.2, prepared by sequential impregnation of Mo and K onto the AC support.

Differential thermal analysis (DTA)

The DTA experiments were carried out on a CRY-1P thermal analyzer (Shanghai Balance Instruments, P. R. China). The sample was heated in flowing N_2 (40 mL/min) from room temperature to $800^\circ C$ at a steady rate of $10^\circ C$ /min. The DTA curves were recorded by using a desktop chart recorder. The reference sample was α - Al_2O_3 , and the sample size used was usually 15 mg.

Temperature-programmed reduction (TPR)

The TPR experiments were conducted on an apparatus constructed from a Hewlett-Packard 5890 gas chromatograph and an external furnace with a temperature programmer. The sample to be analyzed was placed in a quartz U-tube reactor and surrounded with quartz chips. The reactor was heated using the furnace, which was controlled by the temperature programmer. The exit gas stream from the reactor passed through a cold trap filled with a mixture of dry ice and acetone and thence to a thermal conductivity detector (TCD) in the gas chromatograph, where the H_2 content of the stream was monitored.

Approximately 120 mg of sample was used for each experiment. To remove any volatile impurities adsorbed on the surface, the sample was first preheated in pure Ar (30 mL/min) at $250^\circ C$ for about 1h, followed by cooling to room temperature in flowing Ar. The atmosphere was then switched to a H_2 /Ar mixture (the same flow rate with a H_2 /Ar molar ratio of 1/9), and the TPR experiment was started. The temperature for a TPR experiment was usually ramped from room temperature to $850^\circ C$ at a fixed rate of $10^\circ C$ /min, and was then held at $850^\circ C$ for about 30min. A Hewlett-Packard computer was used for data acquisition and processing. The TPR profiles were analyzed by deconvoluting them (assuming a Gaussian-type function) by using a PeakFit software from Jandel Scientific. In order to quantify the H_2 consumption so as to estimate the reducing extent of the catalysts after reduction, the TCD was calibrated by the stoichiometric reduction of ultra-pure CuO (99.9999% CuO). Molybdenum valences are then calculated assuming that the initial valence value of Mo is +6.

Catalytic reaction

The catalytic performance for alcohol synthesis was tested on a computer-controlled high-pressure downstream microreactor system. Typically, 0.5g of catalyst and 3g of crushed quartz chips were mixed together and placed in the center of the stainless steel tubular reactor, with Pyrex beads upstream and downstream of the catalyst-quartz mixture. Prior to reaction, the catalyst under test was first reduced *in situ* in flowing H₂ (50mL/min for 0.5g catalyst) at 400°C and atmospheric pressure for 12h. Detailed description for the reactor system and the reaction procedure was given elsewhere [45].

The reaction product stream was sampled immediately downstream of the reactor using a high-temperature high-pressure sampling valve. The products were then analyzed on-line using a HP5890 gas chromatograph (GC). Gas lines from the sampling valve to the GC were always kept at 250°C (the same temperature as for the GC injector) to avoid product condensation. The carrier gas flow containing the reaction products is split between two columns in the GC: a HayeSep-DB packed column and a J&W DB-Wax capillary column. The packed column is connected to a TCD, which provides quantitative analysis for N₂ (an internal standard) as well as CO, CO₂ and H₂O; hydrogen is separated but cannot be measured satisfactorily. The capillary column is connected to a flame ionization detector (FID) for separation and analysis of organic products (including all of C₁ to C₇ alcohols, and C₁-C₆ hydrocarbons as a single peak). The attribution of the GC peaks is facilitated by injecting standards and matching the retention times. The liquid phase was collected at room temperature and analyzed by a Varian gas chromatograph-mass spectrometer (GC-MS) using a J&W DB-Wax capillary column, to further confirm the attribution of the on-line GC peaks. More details for product analysis can be seen elsewhere [45].

The conversion of carbon monoxide is calculated from the change of the relative concentration of CO to N₂ (assuming N₂ is not reacted). Selectivity of products is based on CO₂-free carbon atoms. This is commonly adopted in literatures [41, 52].

References

1. Massoth, F.E. Characterization of molybdena catalysts. *Adv. Catal.* **1978**, *27*, 265.
2. Murchison, C. B.; Murdick, D. A. Process for producing C₂-C₄ hydrocarbons from carbon monoxide and hydrogen. *US Patent 4,151,190* **1979**, to The Dow Chemical Company.
3. Saito, M.; Anderson, R. B. *J. Catal.* **1980**, *63*, 438.
4. Saito, M.; Anderson, R. B. *J. Catal.* **1981**, *67*, 296.
5. Inoue, M.; Miyake, T.; Takegami, Y.; Inui, T. Direct alcohol synthesis from syngas on ruthenium-molybdenum-sodium/alumina catalysts: effects of physical properties of alumina supports *Appl. Catal.* **1987**, *29*, 285.
6. Tatsumi, T.; Muramatsu, A.; Tominaga, H. Supported molybdenum catalysts for alcohol synthesis from CO-H₂. *Appl. Catal.* **1987**, *34*, 77.

7. Tatsumi, T.; Muramatsu, A.; Fukunaga, T.; Tominaga, H. Nickel-promoted molybdenum catalysts for synthesis of mixed alcohols. In *Proc. 9th Intern. Congr. Catal.*, Phillips, M. J.; Ternan, M. Eds.; The Chemical Institute of Canada: Ottawa, **1988**; Vol. II, p 618.
8. Tatsumi, T.; Muramatsu, A.; Tominaga, H. Molybdenum catalysts for synthesis of mixed alcohols from synthesis gas. *Sekiyu Gakkaishi (J. Jpn. Petrol. Inst.)*, **1992**, 35, 233.
9. Murchison, C. B.; Murdick, D. A. Syngas to LPG over moly catalysts. *Hydrocarbon Processing*, **1981**, 60, 159.
10. Murchison, C. B.; Conway, M. M.; Stevens, R. R.; Quarderer, G. J. Mixed alcohols from syngas over moly catalysts. In *Proc. 9th Intern. Congr. Catal.*; Phillips, M. J.; Ternan, M. Eds.; The Chemical Institute of Canada: Ottawa, **1988**; Vol. II, p 626.
11. Conway, M. M.; Murchison, C. B.; Stevens, R. R. Alcohols from synthesis gas. (Continuation of European patents 0 170 973 and 0 172 431). *U.S. Patent 4,675,344* **1987**, to The Dow Chemical Company.
12. Stevens, R. R. Process for producing alcohols from synthesis gas. *U.S. Patent 4,752,623* **1988**, to The Dow Chemical Company.
13. Gunturu, A. K.; Kugler, E. L.; Cropley, J. B.; Dadyburjor, D. B. A kinetic model for the synthesis of high-molecular-weight alcohols over a sulfided Co-K-Mo/C catalyst. *Ind. Engr. Chem. Res.* **1998**, 37, 2107.
14. Klier, K.; Herman, R. G.; Simmons, G. W.; Lyman, C. E.; Santiesteban, J. G.; Najbar, M.; Bastian, R. *Direct synthesis of alcohol fuels over molybdenum-based catalysts*, US Department of Energy final technical report DOE/PC/80014-T1; Lehigh University, Bethlehem, PA; **1988**.
15. Forzatti, P.; Tronconi, E.; Pasquon, I. Higher alcohol synthesis. *Catal. Rev. - Sci. Eng.* **1991**, 33, 109.
16. Natta, G.; Colombo, U.; Pasquon, I. Direct catalytic synthesis of higher alcohols from carbon monoxide and hydrogen. In *Catalysis*; Emmett, P. H., Ed.; Reinhold: New York, **1957**; Vol. 5, Chapter 3, p 131.
17. Smith, K.; Anderson, R. B. A chain growth scheme for the higher alcohol synthesis. *J. Catal.* **1984**, 85, 428.
18. Villa, P. L.; Forzatti, P.; Buzzi-Ferraris, G.; Garone, G.; Pasquon, I. Synthesis of alcohols from carbon oxides and hydrogen. I. Kinetics of the low-pressure methanol synthesis. *Ind. Eng. Chem. Process Des. Dev.* **1985**, 24, 12.
19. Villa, P. L.; Del Piero, G.; Cipelli, A.; Lietti, L.; Pasquon, I. Synthesis of alcohols from carbon oxides and hydrogen. III. Copper-manganese-titanium-potassium oxide systems. *Appl. Catal.* **1986**, 26, 161.
20. Villa, P. L.; Del Piero, G.; Lietti, L.; Garagiola, F.; Mologni, G.; Tronconi, E.; Pasquon, I. Synthesis of alcohols from carbon oxides and hydrogen. VI. Zinc and titanium oxides: preparation and catalytic activity. *Appl. Catal.* **1987**, 35, 47.

21. Forzatti, P.; Cristiani, C.; Ferlazza, N.; Lietti, L.; Tronconi, E.; Villa, P. L.; Pasquon, I. Synthesis of alcohols from carbon oxides and hydrogen. VII. Preparation, activation and catalytic behavior of a zinc-manganese-chromium-potassium oxide catalyst. *J. Catal.* **1988**, *111*, 120.
22. Klier, K.; Herman, R. G.; Young, C. W. Direct synthesis of 2-methyl-1-propanol. *Prepr. Pap. - Am. Chem. Soc., Div. Fuel Chem.* **1984**, *29*, 273.
23. Nunan, J. G.; Bogdan, C. E.; Klier, K.; Smith, K. J.; Young, C. W.; Herman, R. G. Higher alcohol and oxygenate synthesis over cesium-doped copper/zinc oxide catalysts. *J. Catal.* **1989**, *116*, 195.
24. Nunan, J. G.; Herman, R. G.; Klier, K. Higher alcohol and oxygenate synthesis over cesium-doped copper/zinc oxide catalysts. Higher alcohol and oxygenate synthesis over cesium/copper/zinc oxide/M₂O₃ (M=aluminum, chromium) catalysts. *J. Catal.* **1989**, *116*, 222.
25. Klier, K.; Herman, R. G.; Simmons, G. W.; Nunan, J. G.; Smith, K. J.; Bogdan, C. E.; Himelfarb, P. B. *Direct synthesis of 2-methyl-1-propanol/methanol fuels and feedstocks*, US Department of Energy final technical report DOE/PC/70021-T1-Rev. 1; Lehigh University, Bethlehem, PA; **1988**.
26. Kaplan, L. Promoting the catalytic process for producing polyhydric alcohols. *Ger. Offen.* *2,643,913*, **1977**, to Union Carbide Corporation.
27. Kaplan, L. Novel solvents for the catalytic process for making polyhydric alcohols. *Ger. Offen.* *2,743,630*, **1978**, to Union Carbide Corporation.
28. Kaplan, L. Promoting n-propyl alcohol formation with vanadium compounds. *US Patent* *4,151,192*, **1979**, to Union Carbide Corporation.
29. Kaplan, L. Catalytic process for producing polyhydric alcohols. *Eur. Patent Appl.* *6,634*, **1980**, to Union Carbide Corporation.
30. Dombek, B. D. *J. Am. Chem. Soc.* **1980**, *102*, 6855.
31. Dombek, B. D. Process for producing alcohols. *Eur. Patent Appl.* *13,008*, **1980**, to Union Carbide Corporation.
32. Dombek, B. D. *ACS Symp. Ser.* **1981**, *152*, 213.
33. Dombek, B. D. *J. Am. Chem. Soc.* **1981**, *103*, 6508.
34. Catalytica Associates, Inc. *Synthesis of methanol, glycols, higher alcohols, and other oxygenates from CO/H₂*, Multiclient Study No. 4162; May **1983**, p 110.
35. Watson, P. R.; Somorjai, G. A. The hydrogenation of carbon monoxide over rhodium oxide surface. *J. Catal.* **1981**, *72*, 347.
36. Inoue, M.; Miyake, T.; Takegami, Y.; Inui, T. Alcohol synthesis from syngas on ruthenium-based composite catalysts. *Appl. Catal.* **1984**, *11*, 103.
37. Anderson, R. B. Nitrided iron catalysts for the Fischer-Tropsch synthesis in the eighties. *Catal. Rev. - Sci. Eng.* **1980**, *21*, 53.
38. Sugier, A.; Freund, E. Saturated and straight chain alcohols from synthesis gas. *US Patent* *4,122,110*, **1978**, to The Institut Francais du Petrole.

39. Santiesteban, J. G.; Bogdan, C. E.; Herman, R. G.; Klier, K. Mechanism of C₁ – C₄ alcohol synthesis over alkali/MoS₂ and alkali/Co/MoS₂ catalysts. In *Proc. 9th Intern. Congr. Catal.*; Phillips, M. J.; Ternan, M. Eds.; The Chemical Institute of Canada: Ottawa, **1988**; Vol. II, p 561.
40. Duan, L.; Zhang, O.; Ma, S.; Li, S.; Xie, Y. The role of K₂CO₃ and the structural state of K⁺ in Mo-based sulfur-tolerant catalysts for alcohol synthesis. *J. Mol. Catal. (China)*. **1990**, *4*, 208.
41. Yang, Y.; Lin, G.; Huang, H.; Zhang, H. Preparation of Mo-based sulfur-tolerant catalysts for alcohol synthesis from syngas. *J. Fuel. Chem. Technol.* **1993**, *21*, 1.
42. Bian, G.; Jiang, M.; Fu, Y.; Omata, K.; Fujimoto, K. Effect of preparation conditions and supports upon catalytic properties of sulfided K-Mo catalysts used for mixed alcohol synthesis from syngas. *J. Fuel. Chem. Technol.* **1993**, *21*, 350.
43. Xie, Y.; Naasz, B. M.; Somorjai, G. A. Alcohol synthesis from CO and H₂ over molybdenum sulfide. *Appl. Catal.* **1986**, *27*, 233.
44. Fu, Y.; Fujimoto, K.; Lin, P.; Omata, K.; Yu, Y. Effect of calcination conditions of the oxidized precursor on the structure of a sulfided K-Mo/ γ -Al₂O₃ catalyst for mixed alcohol synthesis. *Appl. Catal. A: General*, **1995**, *126*, 273.
45. Liu, Z.; Li, X.; Close, M. R.; Kugler, E. L.; Petersen, J. L.; Dadyburjor, D. B. Screening of alkali-promoted vapor-phase-synthesized molybdenum sulfide catalysts for the production of alcohols from synthesis gas. *Ind. Eng. Chem. Res.* **1997**, *36*, 3085.
46. Li, X.; Feng, L.; Liu, Z.; Zhong, B.; Dadyburjor, D. B.; Kugler, E. L. Higher alcohols from synthesis gas using carbon-supported doped molybdenum-based catalysts. *Ind. Eng. Chem. Res.* **1998**, *37*, 3853.
47. Jiang, M.; Bian, G.-Z.; Fu, Y.-L. Effect of the K-Mo interaction in K-MoO₃/ γ -Al₂O₃ catalysts on the properties for alcohol synthesis from syngas. *J. Catal.* **1994**, *146*, 144.
48. Lee, J. S.; Kim, S.; Lee, K. H.; Nam, I.-S.; Chung, J. S.; Kim, Y. G.; Woo, H. C. Role of alkali promoters in K/MoS₂ catalysts for CO-H₂ reactions. *Appl. Catal. A: General*, **1994**, *110*, 11.
49. Quarderer, G.J.; Cochran, K. A. Process for producing mixed alcohols from hydrogen and carbon monoxide. *Eur. Patent 0119609*, **1984**, to The Dow Chemical Company.
50. Stevens, R. R. Alcohols from synthesis gas. *Eur. Patent 0172431*, **1986**, to The Dow Chemical Company.
51. Kinkade, N. E. Alcohols from carbon monoxide and hydrogen using an alkali-molybdenum sulfide catalyst. *Eur. Patent 0149256*, **1985**, to Union Carbide Corporation.
52. Alyea, E. C.; He, D.; Wang, J. Alcohol synthesis from syngas. I. Performance of alkali-promoted Ni-Mo(MOVS) catalysts. *Appl. Catal. A: General*, **1993**, *104*, 77.
53. Storm, D. A. The production of higher alcohols from syngas using potassium promoted Co/Mo/Al₂O₃ and Rh/Co/Mo/Al₂O₃. *Topics in Catal.* **1995**, *2*, 91.
54. Duchet, J. C.; van Oers, E. M.; de Beer, V. H. J.; Prins, R. Carbon-supported sulfide catalysts. *J. Catal.* **1983**, *80*, 386.
55. Feng, L.; Li, X.; Kugler, E. L.; Dadyburjor, D. B. A temperature-programmed-reduction study on alkali-promoted, carbon-supported molybdenum catalysts. *J. Catal.* **2000**, *190*, 1.

56. Li, M.; Cheng, Y. W.; Ye, X. L. A thermal analysis study on the decomposition and reduction of unsupported and supported ammonium molybdate. *Chinese Chem. World*, **1998**, *39*, 628.
57. Ratnasamy, P.; Mehrotra, R. P.; Ramaswamy, A. V. Interaction between the active components and support in cobalt-molybdenum-alumina systems. *J. Catal.* **1974**, *32*, 63.
58. Dandekar, A.; Baker, R. J. K.; Vannice, M. A. Characterization of activated carbon, graphitized carbon fibers and synthetic diamond powder using TPD and DRIFTS. *Carbon*, **1998**, *36*, 1821.
59. Arnoldy, P.; De Jonge, J. C. M.; Moulijn, J. A. *J. Phys. Chem.* **1985**, *89*, 4517.
60. Brito, J. L.; Laine, J.; Pratt, K. C. *J. Mater. Sci.* **1989**, *24*, 425.
61. Walker, P. L., Jr.; *Chemistry and Physics of Carbon*, Marcel Dekker: New York, **1970**; Vol.6.
62. Kelemen, S. R.; Freund, H.; Mims, C. A. The dependence of water adsorption and reaction on the structure of the carbon substrate. *J. Vac. Sci. Technol.* **1984**, *A(2)*, 987.
63. Kelemen, S. R.; Freund, H.; Mims, C. A. The interaction of potassium hydroxide with clean and oxidized carbon surfaces. *J. Catal.* **1986**, *97*, 228.
64. Otake, Y.; Jenkins, R. G. Characterization of oxygen-containing surface complexes created on a microporous carbon by air and nitric acid treatment. *Carbon*, **1993**, *31*, 109.
65. Kelemen, S. R.; Mims, C. A. The interaction of potassium hydroxide with basal surface of graphite. *Surf. Sci.* **1983**, *133*, 71.
66. Rajagopal, S.; Marini, H. J.; Marzari, J. A.; Miranda, R. Silica-alumina-supported acidic molybdenum catalysts – TPR and XRD characterization. *J. Catal.* **1994**, *147*, 417.
67. Arnoldy, P.; Franken, M. C.; Scheffer, B.; Moulijn, J. A. Temperature-programmed reduction of cobalt monoxide-molybdena/alumina catalysts. *J. Catal.* **1985**, *96*, 381.
68. Watson, P. R.; Somorjai, G. A. The formation of oxygen-containing organic molecules by the hydrogenation of carbon monoxide over a lanthanum rhodate catalyst. *J. Catal.* **1982**, *74*, 282.